Appl. Phys. 19, 153–163 (1979)

Applied Physics

Diffraction Efficiency and Energy Transfer During Hologram Formation in Reduced $KNbO_3$

*A. Krumins** and *P. Günter*

Laboratory of Solid State Physics, Swiss Federal Institute of Technology, CH-8093 Zürich, Switzerland

Received 29 November 1978/Accepted 12 February 1979

Abstract. Volume phase-hologram formation by the photorefractive effect in $KNbO_3$ is accompanied by a stationary energy transfer between writing beams. The change in energy transfer by applying an electric field on the reduced crystals is shown to be due to an efficient increase in migration length which can reach values comparable or larger than the fringe spacing. It is demonstrated that photovoltaic contribution to the diffraction efficiency and energy transfer is rather small in reduced $KNbO_3$ and that diffusion of photogenerated free holes is the dominant charge transport for the photorefractive effect in unbiased crystals. The experimental results for diffraction efficiency and energy transfer as a function of grating spacing, electric field, light intensity and temperature is well described by a recent theory of Kukhtarev and Vinetskii.

PACS: 42.30.–d, 42.40.–i, 42.70.–a, 72.40.tw, 78.20.Jq.

Recording of volume phase-holograms by the photorefractive effect in electrooptic crystals has been intensively studied in recent years [1, 2]. Ferroelectric materials as $LiNbO_3$ [2], $BaTiO_3$, [3] SBN [4], $LiTaO_3$ [5] and $KNbO_3$ [6] as well as photoconductive nonferroelectrics as KTN [7] and $Bi_{12}SiO_{20}$ and $Bi_{12}GeO_{20}$ [8] have been used as storage materials. The characteristic parameters (photosensitivity, diffraction efficiency and storage time of the holograms) of the photorefractive effect in different materials have been shown to be mainly determined by the different charge transport processes (photovoltaic drift, photoconductivity and diffusion) of the photoexcited carriers. Trapping of these charges in dark areas leads to space-charge fields between bright and dark areas of the picture to be recorded. The changes in refractive index (phase-hologram formation) are then due to the electrooptic effect driven by these space-charge fields.

The characteristic transport length $\mu\tau E$ and $(D\tau)^{1/2}$ (where μ is the mobility, τ is the lifetime before retrapping, and D is the diffusivity) have been shown to be short compared with the grating spacing in most of the ferroelectric materials. Therefore many cycles of photoexcitation, charge transport and trapping are necessary until the charges are finally trapped in dark areas of the hologram. An increase in the operative transport length (up to a certain limit comparable to the fringe spacing of the hologram), which is the case in highly photoconducting materials as KTN [7], $Bi_{12}SiO_{20}$, $Bi_{12}GeO_{20}$ [6], SBN + Ce [9] and as will be shown in this paper also in reduced $KNbO_3$, lead to an increased efficiency in hologram writing.

Recording of thick volume holograms permits the interference of an incident light beam with its own diffracted beam inside the recording material. This effect causes the continuous recording of a new grating that may add to or subtract from the initial grating that is not uniform through the thickness of the material, and which can be phase shifted to the initial grating. The energy redistribution between writing beams due to such a phase shift between the fringe pattern and the recorded grating has been observed in undoped [10, 11] and Fe doped [12] $LiNbO_3$ as well as in $Bi_{12}SiO_{20}$ and $Bi_{12}GeO_{20}$ [8]. Stationary energy

* Permanent address: Institute of Solid State Physics, Latvian State University, SU-226098 Riga, Latvian SSR, UdSSR.

0340-3793/79/0019/0153/$02.20

transfer has been shown to be forbidden if there is a phase shift of zero or π between the interference pattern and the recorded hologram [10, 13]. Transient energy transfer between writing beams during hologram recording has been observed in reduced "undoped" $LiNbO_3$ biased by an external electric field [14]. This effect has been shown to result from a nonstationary phase mismatch of the fringe pattern and the recorded grating, if the two writing beams have different intensities [14]. This beam coupling effect during hologram recording has been suggested to be useful for coherent light beam amplification [11, 14].

A stationary grating shift ($\psi=\pi/2$) arises if diffusion is the dominant recording mechanism [15]. This is the case in unbiased $Bi_{12}SiO_{20}$ and $Bi_{12}GeO_{20}$ [8] and perhaps also in "undoped" $LiNbO_3$ [10, 11]. Charge transport by drift due to an external or "internal" (photovoltaic) field can lead to a change in the phase angle ψ, but only if the Debye length of the carriers is comparable to or larger than the fringe spacing Λ (violation of quasineutrality) [16, 11]. It has been shown that electric fields of up to 20 KV/cm applied to pure [10] and reduced [11] $LiNbO_3$ crystals have no significant influence on the stationary energy transfer; therefore driftinduced grating shift is almost neglectable in this material.

The purpose of this paper is to study photorefraction and energy transfer during hologram formation in reduced $KNbO_3$, where a possible violation of quasineutrality appears [6]. Most of our results will be interpreted in terms of a recent theory of Kukhtarev and Vinetskii [11].

In an earlier work [6] we have shown that the photorefractive effect in $KNbO_3$ is caused by diffusion (if the fringe spacing Λ of the holograms is small), by the photovoltaic effect (in unbiased crystals) and by photoconductivity in an external field E. By varying either the fringe spacing Λ or the electric field E each one of these three charge-transport processes can be made to dominate the other two. This is one reason why $KNbO_3$ is an interesting test material for the existing theories.

Reduced $KNbO_3$ is ideally suited for the experiments mentioned above because of the following reasons:

1) Photoconductivity is very large in these crystals since

2) drift length is comparable to the fringe spacing of visible light holograms.

3) The Maxwell time constants τ are very small ($\tau=20$ ms in the dark and $\tau=1$ ms for an intensity of $I=0.1$ W/cm^2 of 488 nm light), which means that many holograms with different parameters can be recorded in a relatively short time and that the "history" of the sample has no influence on the measurement. The material also suffers no "fatigue" effect as e.g. is the case in $LiNbO_3$.

4) The charge transport by the photovoltaic effect can be neglected in reduced $KNbO_3$, since, due to the large photoconductivity, the photovoltaic field is negligibly small ($E_{pv}\approx 2$ V/cm).

1. Theoretical Considerations

The photorefractive effect and energy transfer must be simultaneously described by a "dynamic" theory, which takes into account any possible changes of the fringe-pattern contrast along the crystal length due to the intensity redistribution between the two writing beams. The dynamic theories by Ninomiya [17], Vahey [18], Magnusson et al. [19] and Moharam et al. [20] are valid only for "short" transport lengths.

The advantage of the theory developed by Kukhtarev and Vinetsky [11] compared to those mentioned above, is the fact that it describes the photorefraction and energy transfer also for long transport lengths. The change of fringe pattern within the crystal depth in this theory is determined by introducing a light intensity dependent dielectric constant ε into the wave equation. The recording medium is supposed to contain donor and trap centers, the electrons are released from donor centers into the conduction band and ionized donors capture the free carriers. An electron, photoexcited into the conductivity band, may shift in an external or internal electric field due to diffusion or photovoltaic effect. Under the steady state conditions the flow of photoexcited electrons is neutralized by the carrier recombination. The resulting field E may be calculated from the Poisson equation.

It follows from self-consistent solutions of the material equations and the wave equation that the field E, modulating the refractive index, has two components: First a parameter A which is the amplitude of the component of the holographic grating, which remains unshifted with respect to the interference pattern; and the second component B, which is a component of the grating, offset by $\pi/2$ with respect to the fringe pattern, describing the energy transfer. It was shown in [11] that the phase mismatch $\psi=\operatorname{arcctg}(A/B)$ remains constant along the hologram depth in the stationary case. For two recording beams having equal intensities ($I_{10}=I_{-10}$), there follows from [10] the simple expression for the phase shift

$$\sin\psi=\frac{I_1-I_{-1}}{4\cdot I_{10}\cdot\sqrt{\eta(1-\eta)}}, \tag{1}$$

where I_I and I_{-I} are steady-state intensities of the diffracted beams, η is the diffraction efficiency.

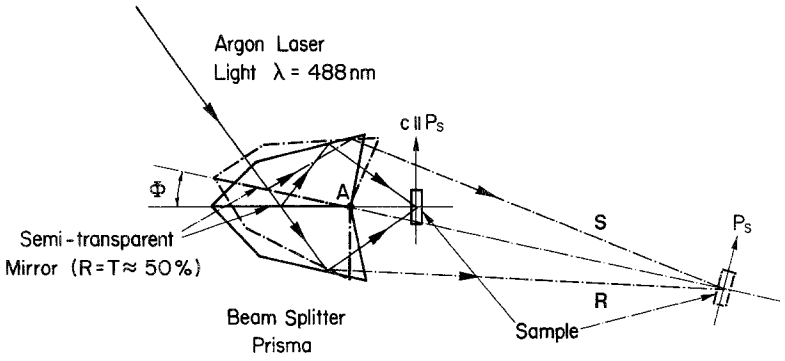

Fig. 1. Experimental configuration for the holographic experiments. (Solid lines: recording with small fringe spacing dashed lines: recording with large fringe spacing

The energy transfer is characterized by the gain Γ which is defined by [11]

$$\Gamma = \frac{1}{l} \ln\left(\frac{I_{-1} \cdot I_{10}}{I_1 \cdot I_{-10}}\right), \tag{2}$$

where l is the crystal thickness; I_{10}, I_{-10} are intensities of two output beams before recording; and I_1, I_{-1} are steady state intensities of diffracted beams.

From [11] the general expressions for the gain Γ and the diffraction efficiency are given by

$$\Gamma = -2 \cdot \delta \cdot B = -2 \cdot \delta \cdot E_T \cdot F \cdot \frac{1 + (E_T/E_q) + (E_0^2/E_T E_q)}{[1 + (E_T/E_q)]^2 + (E_0/E_q)^2} \tag{3}$$

and

$$\eta = \frac{2m \exp\frac{\Gamma \cdot l}{2} [\mathrm{ch}(\Gamma l/2) - \cos(\delta A l)]}{(1+m)[1 + m \exp(r \cdot l)]}, \tag{4}$$

where

$$\delta = \pi \cdot n_3 \cdot r_{33}/\lambda_0 \cos(\theta_0/2), \quad m = I_{10}/I_{-10};$$

n_3 is refractive index, r_{33} is the effective electrooptic coefficient, $\lambda_0 = 632.8$ nm, θ_0 is the angle for recording beam, $F = 1$ or 0.5 for the linear or quadratic recombination case, E_T is the diffusion field, E_0 the applied field, E_q the maximal field of the volume space-charge which corresponds to complete separation of positive and negative charges with the period of the holographic gratings.

The maximal space-charge field is given by [11]

$$E_q = \frac{2e}{\varepsilon_{33}\varepsilon_0} \Lambda v, \tag{5}$$

where $v = N_A$ for linear recombination and $v = 2n_0$ for quadratic recombination, N_A is the concentration of empty donors, n_0 the carrier concentration.

For small gain and small phase changes

$$(\Gamma \cdot l/2 \ll 1, \pi \Delta n l/\lambda_0 \cos(\theta_0/2) \ll 1 \text{ or } \eta \ll 1)$$

the expression (4) for the diffraction efficiency can be simplified to [11]

$$\eta = \frac{2m}{(1+m)^2} \frac{(\delta \cdot F \cdot E_T \cdot l)^2 [1 + (E_0/E_T)^2]}{\{[1 + (E_T/E_q)]^2 + (E_0/E_q)^2\}}. \tag{6}$$

2. Experiment

The main purpose of this experiment was the investigation of volume phase-hologram formation in reduced $KNbO_3$. It has been shown earlier [6] that the experimental parameters (electric field fringe spacing) can be choosen such that either photoconductivity or diffusion is the dominant charge transport. Measurements of holographic diffraction efficiency η and energy transfer between writing beams (gain) Γ [11] had to be measured as a function of the electric field E_0, fringe spacing Λ, total light intensity I_0, intensity ratio between writing beams m and temperature T.

The holograms were recorded by the interference of two light beams. For the measurement of the fringe-spacing dependence the two interfering light beams were produced by a single beam splitter, as shown in Fig. 1. In this configuration we always had exactly the same light path for the interfering beams and the possibility of continuously changing the fringe spacing from $\Lambda = 1\,\mu$m to $\Lambda = 10\,\mu$m by just rotating the beam splitter and moving the sample to the place were there is interference. In all our measurements we used the $\lambda = 488$ nm line of a Lexel Ar ion laser (Type 95) which had a maximum intensity of 1 W. For the measurement of the light intensity or beam ratio dependence the beams have been attenuated by an optical attenuator (Newport Res. Typ 925B) which had very low beam distortions even at the highest power densities of the direct Ar beam. The interfering beams were polarized in the plane of incidence, the c axis of the crystal was perpendicular to the bisector of the incident beams. Recording experiments were also performed with variable electric fields up to 7 kv/cm applied parallel to the polar c-axis, using silver-paste electrodes, the diffrac-

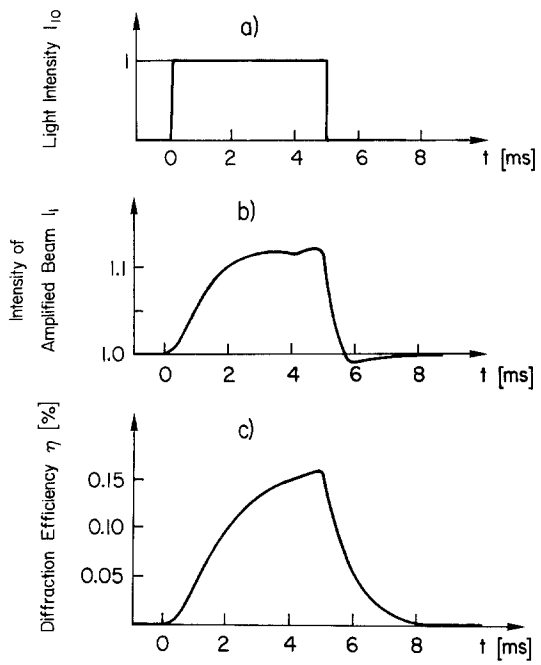

Fig. 2a–c. Time dependence of recording light beam I_{10} (a), of coupled beam (b) and diffracted probe beam for $\Lambda = 1.8\,\mu m$, $I_{10} = 0.5\,W/cm^2$, $E_0 = 0$ and $m \simeq 1$

tion efficiency η was continuously monitored using a low-power He–Ne laser under Bragg incidence with the same polarization as the Ar laser. Both incident and transmitted intensities of writing beams (Ar) and diffracted probe beams (He–Ne) were measured with a "United Detector Technol. Inc." photometer (Typ 80X) or a photomultiplier.

We used nominally pure crystals of $KNbO_3$ which had a Fe concentration of 46 ± 11 ppm. The crystals were grown in our laboratory by Flückiger and Arend [21]. Reduction was performed electrochemically by annealing them in silicon oil at 200 °C during 100 h, since it was not advisable to heat them above the two strongly first-order phase transitions at 217 °C and 430 °C. The optical spectra of oxidized and reduced crystals have been reported in [22]. A pronounced maximum at 2.55 eV appears in the spectrum of the reduced crystal. The absorption coefficient for $\lambda = 488$ nm was increased to $\alpha = 3.8\,cm^{-1}$. The dimensions of the prismatic single domain crystal were $a \times b \times c = 6 \times 3 \times 3.3\,mm^3$. The aperture of the crystal holder permitted recording in an area of $4 \times 3.3\,mm^2$.

Since the photorefractive effect in $KNbO_3$ is determined by many different variables [6, 20] we would like to quote here the detailed experimental conditions used throughout this measurements:

1) Electrical conditions: A constant voltage was applied to the crystal if $E_0 \neq 0$ and the sample was short-circuited if $E_0 = 0$.

2) The diameter of the interference pattern was larger than the crystal length, therefore "large-scale" space-charge fields can be neglected [20].

3) Heating up of the sample by the light beams was measured by a thermocouple in contact with the crystal, for $T < 120$ °C. Temperature changes had to be smaller than 5 °C in order to yield no oscillations of the diffraction efficiency due to multiple internal reflections [23].

4) The room temperature dark conductivity σ_d of our sample was $\sigma_d \approx 10^{-12}\,(\Omega cm)^{-1}$ and the photoconductivity σ_p for $I_0 = 0.05\,W/cm^2$ of $\lambda = 488$ nm light was $\sigma_p = 1150 \cdot \sigma_d$ [24].

3. Results

In this section we list our experimental results for diffraction efficiency and energy transfer which we will discuss in the next section. Hologram formation in reduced $KNbO_3$ at $I_0 \approx 1\,W/cm^2$ is about 10^4 times faster than in pure $LiNbO_3$ [10] due to the much higher conductivity. All of the following results on diffraction efficiency apply for steady state, which for this reason was reached very rapidly (typically 2 to 100 ms). The direction of energy transfer in reduced $KNbO_3$ was from S to R (see Fig. 1), just the opposite from that in $LiNbO_3$ [10]. For any intensity ratio m of the two beams, any electric field parallel to the polar direction or smaller than E_c in the reverse direction, and for any temperature, the direction of energy transfer was always the same. No transient energy transfer like in $LiNbO_3$ [14] has been detected for small modulation ratios m and $E_0 \neq 0$. In analogy to the results observed in $LiNbO_3$ [10], the time constants for the energy transfer were faster than for the diffraction efficiency in $KNbO_3$, too (Fig. 2).

3.1. Fringe Spacing Dependence of Diffraction Efficiency η and Gain Γ

Without an external electric field the diffraction efficiency decreases as Λ^{-2} with increasing grating spacing Λ for $\Lambda = 1.5 \ldots 10\,\mu m$ (Fig. 3). This is the expected behaviour for the diffusion case. Similar results have been obtained in $BaTiO_3$ [3], Fe-doped [25] and pure [11] $LiNbO_3$ and Fe doped $KNbO_3$ [6]. For increasing electric fields the decrease in diffraction efficiency becomes smaller and smaller as photoconductivity becomes dominant in comparison to diffusion. For $E_0 = 7\,kV/cm$ diffusion is negligable and the diffraction efficiency becomes independent of fringe spacing Λ for $\Lambda > 3\,\mu m$.

The gain Γ is inversely proportional to the fringe spacing for $E_0 = 0$ (Fig. 4). This behaviour has also

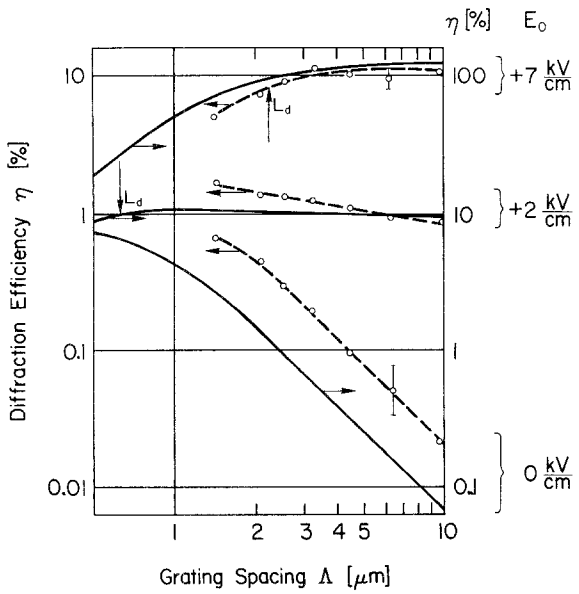

Fig. 3. Diffraction efficiency versus grating spacing for different external electric field for ($I_0 = 1\,W/cm^2$ and $m \simeq 1$, solid lines: theoretical according to (6), dashed lines: experiment)

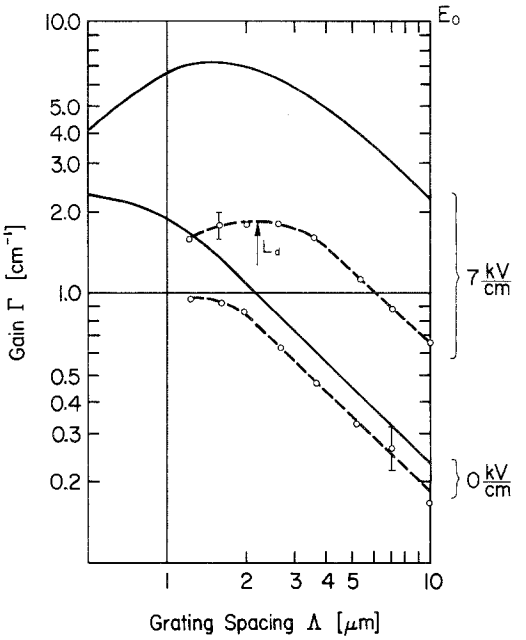

Fig. 4. Gain Γ versus grating spacing Λ for different external electric fields for ($I_0 = 1\,W/cm^2$ and $m \simeq 1$, solid lines: theoretical, according to (3), dashed lines: experiment)

been observed in pure $LiNbO_3$ [11]. However in $KNbO_3$ the gain increases for increasing electric fields (increase of photoconductivity). For $E_0 = 7\,kV/cm$ the gain first increases and decreases again inversely proportional to the fringe spacing Λ for $\Lambda > 3\,\mu m$.

3.2. *Electric Field Dependence of Diffraction Efficiency η and Gain Γ*

It has been shown in an earlier paper [6] that the diffraction efficiency in Fe doped $KNbO_3$ can be drastically in- or decreased by applying an electric field on the sample. Depending on the direction of the electric field (relative to the $\pm$ polar axis) the photocurrents have the same or the contrary direction to the photovoltaic currents. In reduced $KNbO_3$ the situation is different, insofar as the photovoltages are very small and photoconductivity is very large. The electric field dependence of the diffraction efficiency therefore becomes completely symmetric along the $\pm E_0$-axis around $E_0 = 0$ (Fig. 5). This result is similar the one in other photoconductive electro-optic but non-ferroelectric materials as, e.g., in $Bi_{12}SiO_{20}$ or $Bi_{12}GeO_{20}$ [8].

The electric field dependence of the gain Γ has been plotted in Fig. 6. By applying an electric field $E_0 = 7\,kV/cm$ the gain is increased by a factor of three or four for a fringe spacing $\Lambda = 1\,\mu m$ and $\Lambda = 10\,\mu m$, respectively. In ferroelectrics with a relatively small photoconductivity, e.g. in pure [10] and reduced [11] $LiNbO_3$ no change in gain Γ has been measured for electric field strengths up to 30 kV/cm. The gain Γ was symmetrical along the $\pm E_0$ axis with respect to $E_0 = 0$ and the expected behaviour $\Gamma \sim E_0^2$ was more pronounced for large grating spacings [11].

3.3. *Diffraction Efficiency η and Gain Γ as a Function of the Intensity Ratio of Writing Beams*

The change of the intensity ratio of the writing beams led to considerable changes in the diffraction efficiency (Fig. 7a). The behaviour is approximately symmetrical with respect to $m = 1$ and maximum efficiency corresponds to the best contrast of the fringe pattern. For reduced $LiNbO_3$ with $\Gamma \sim 10\,cm^{-1}$ it has been shown that $\eta(m)$ is not symmetrical with respect to $m = 1$ [11].

The intensity ratio dependence of the gain Γ is seen to be relatively weak in Fig. 7b. A change of m by two orders of magnitude leads to less than a 1.5 fold change in Γ.

3.4. *Light Intensity Dependence of Diffraction Efficiency η and Gain Γ*

The intensity dependence of diffraction efficiency for this crystal has already been reported in [6]. The

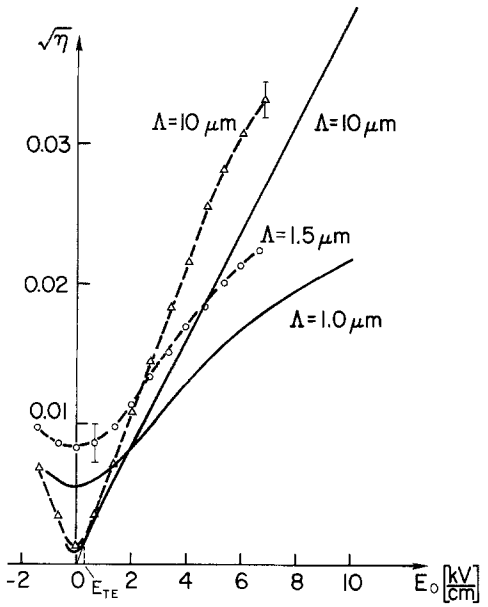

Fig. 5. Square root of diffraction efficiency versus external electric field for different grating spacings. $I_0 = 1\,\mathrm{W/cm^2}$, $m \simeq 1$, solid lines: theoretical according to (6) (relative units), dashed lines: experiment

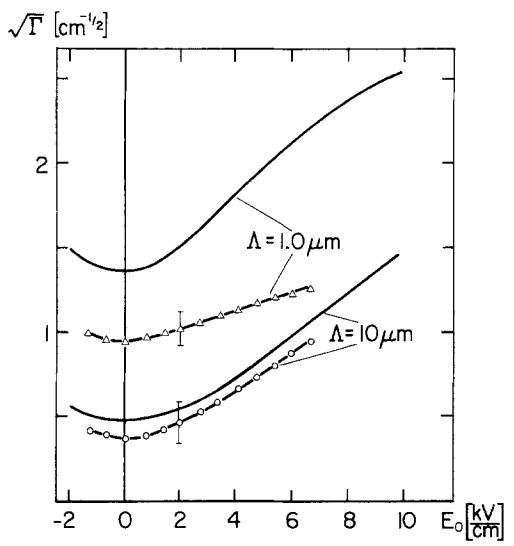

Fig. 6. Square root of gain Γ versus external electric field for different grating spacings Λ for $I_0 = 1\,\mathrm{W/cm^2}$ and $m \simeq 1$ (solid lines: theoretical according to (3), dashed lines: experiment)

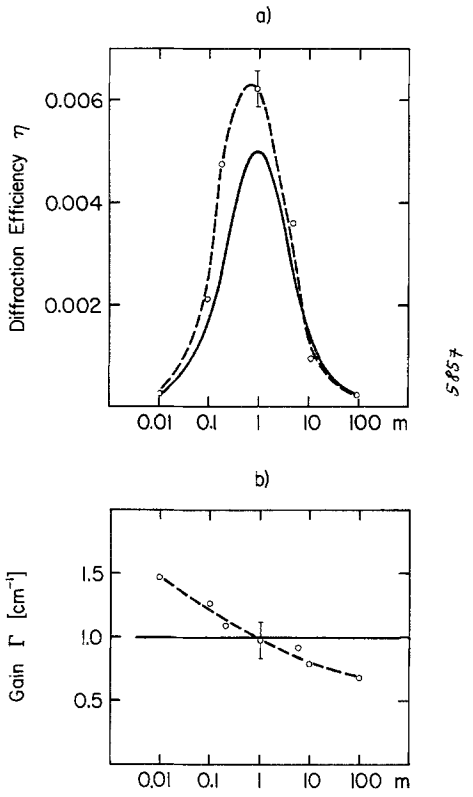

Fig. 7a and b. The diffraction efficiency (a) and gain Γ (b) versus intensity ratio m of writing beams for $\Lambda = 2\,\mu\mathrm{m}$ and $I_0 = 1\,\mathrm{W/cm^2}$ (solid lines: theoretical, dashed lines: experiment)

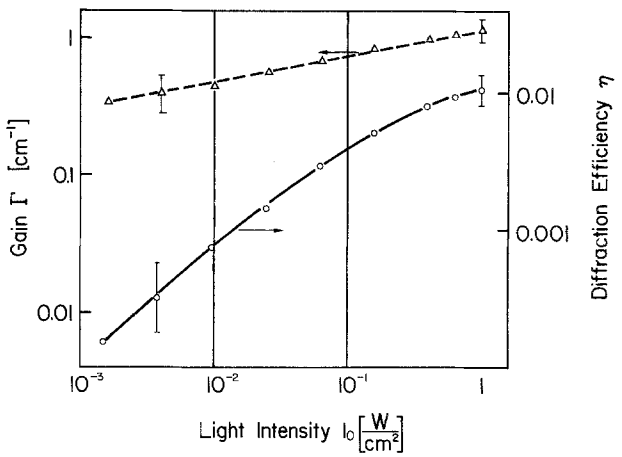

Fig. 8. Diffraction efficiency (solid line), and gain Γ (dashed line) versus total intensity of the writing beams for $m \simeq 1$, $\Lambda = 1.6\,\mu\mathrm{m}$ and $E_0 = 0$

diffraction efficiency increases monotonically for small writing intensities where dark conductivity dominates the photoconductivity. Above $I_0 = 1\,\mathrm{W/cm^2}$ $\eta(I_0)$ saturates, because the dark currents are much smaller than the photocurrents in this regime (Fig. 8).

The gain Γ shows only a weak intensity dependence (Fig. 8) which is given by the approximate relation $\Gamma \sim I_0^{0.2}$. Both diffraction efficiency and gain dependences as a function of I_0 become similar if E_0, Λ or m are changed.

3.5. *Temperature Dependence of Diffraction Efficiency η and Gain Γ*

Undoped $KNbO_3$ is orthorhombic point group mm 2 between $-45\,°C$ (transformation to the rhombohedral phase; point group 3 m) and 217 °C (transformation to the tetragonal phase; point group 4 mm) [26]. Our measurements were performed in the orthorhombic phase only and from room temperature up to 200 °C.

The measurement of diffraction efficiencies above 100 °C was complicated by the fact that crystals were heated up by $\lambda = 488$ nm light absorption, so that the diffraction efficiency decreased. To avoid heating up of the sample only 5 ms light pulses, produced with a mechanical chopper, were projected into the crystal.

The temperature dependence of the steady-state diffraction efficiency for $E_0 = 0$ and $E_0 = 3\,kV/cm$ is shown in Fig. 9. The diffraction efficiency for zero applied field has two peaks near 70 °C and 170 °C. The first one is probably due to changes in conductivity. However our results cannot completely be interpreted by the results of measurements of the temperature dependences of these properties [24]. With an external electric field the diffraction efficiency η first decreases but shows the same peak near 170 °C. Therefore we suggest that this peak might be connected with the appearance of photodomains, as has already been observed in $BaTiO_3$, too [27]. The decrease of diffraction efficiency with increasing temperature has also been observed earlier in other ferroelectric materials as in Fe doped $LiNbO_3$ [28, 29] and in (Ba, Sr) NbO_3 [30].

The temperature dependence of the gain Γ both for $E_0 = 0$ and $E_0 \neq 0$ is much weaker than for the diffraction efficiency (Fig. 10). Some temperature hysteresis has been observed for both $\eta(T)$ and $\Gamma(T)$.

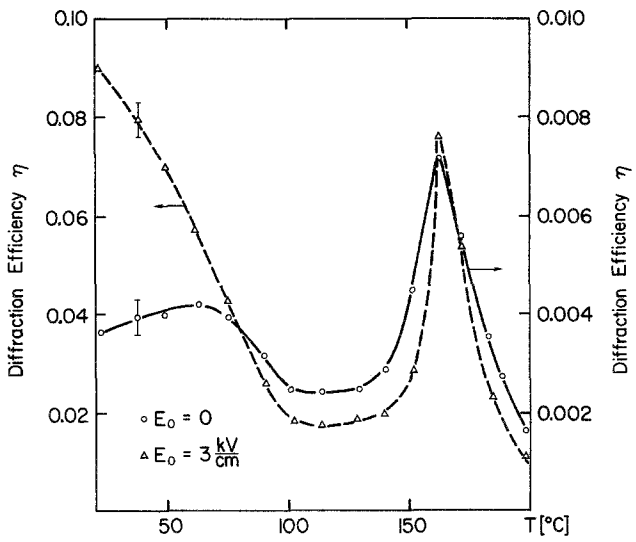

Fig. 9. Diffraction efficiency versus temperature for different external electric fields: $E_0 = 0$ (solid line), $E_0 = 3\,KV/cm$ (dashed line), with $m = 1$, $\Lambda = 4\,\mu m$, and $I_0 = 1\,W/cm^2$, ($\tau = 5$ ms)

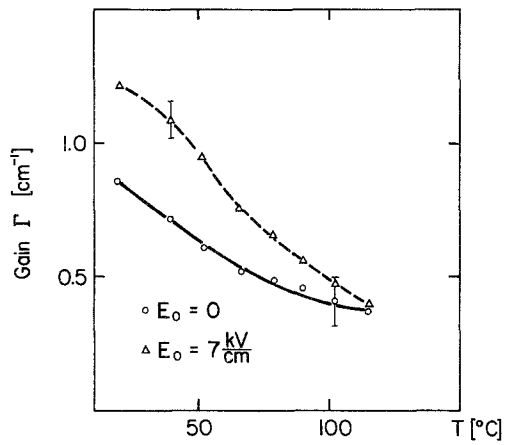

Fig. 10. Gain Γ versus temperature for different external electric fields E_0: $E_0 = 0$ (solid line), $E_0 = 7\,KV/cm$ (dashed line), with $m = 1$, $\Lambda = 2\,\mu m$ and $I_0 = 1\,W/cm^2$

4. Discussion

4.1. *Diffraction Efficiency, Gain and Phase Shift ψ for Diffusion ($E_0 = 0$)*

The presence of beam coupling between writing beams for $m \simeq 1$ (Fig. 2), shows that there must exist a phase shift ψ of the holographic phase grating with respect to the interference pattern. For $\Lambda = 10 \ldots 1\,\mu m$ we get from (1) a value of $\sin\psi = 0.9 \ldots 1.0$. The phase shift is therefore approximatively a quarter of the fringe spacing. This shift is induced by volume space charges due to photoexcited carrier diffusion [15]. The diffusion contribution can be clearly seen in Fig. 4 for $E_0 = 0$ where the drift does not contribute to the charge transport [extrapolation of $\eta^{1/2}(E_0) \to 0$ for $E_0 \to 0$]. The equivalent diffusion field $E_{TE} = 250\,V/cm$, i.e. the field which has to be applied in order to obtain the same diffraction efficiency as by diffusion only, is comparable with the diffusion field $E_T = 2\pi kT/(e\Lambda) = 160\,V/cm$ at $\Lambda = 10\,\mu m$, where k is the Boltzmann constant and e the electronic charge.

Photovoltaic currents have not to be taken into account for our further discussion, since they are much smaller than the photocurrents, even for small applied electric field [34]. The completely symmetric behaviour of $\eta(E_0)$ (Fig. 5) supports this assumption.

The direction of energy transfer is associated with the direction of the shift and the sign of the refractive index changes [10] or operative electrooptic coefficient $r_{33} = (+64 \pm 5) \cdot 10^{-12}\,m/v$ [31].

Since the energy transfer is in the opposite direction to the one in $LiNbO_3$ and since electrons are the dominant carriers in $LiNbO_3$ [32] we conclude that the hologram formation in $KNbO_3$ is produced by the diffusion of photogenerated free holes. Hole conductivity in $KNbO_3$ has already been suggested by thermoconductivity measurements [33]. For the diffusion case, if $E_0=0$ it follows from (6) and (3), that

$$\eta \sim \frac{E_T^2}{[1+(E_T/E_q)]^2} \tag{7}$$

$$\Gamma \sim \frac{E_T}{1+E_T/E_q}. \tag{8}$$

The term in the denominator is larger than unity only if $E_T \approx E_q$ which is the case for small fringe spacings only. Therefore the diffraction efficiency η shown in Fig. 3 saturates for $\Lambda \to 0$. In this region the Debye length $l_D \approx 0.5\,\mu m$ is comparable with the fringe spacing. For larger fringe spacings (7) and (8) gives the following behaviours: $\eta \sim E_T^2 \sim \Lambda^{-2}$ and $\Gamma \sim E_T \sim \Lambda^{-1}$ which are in good agreement with the experiment (Figs. 3 and 4).

4.2. *Diffraction Efficiency, Gain and Phase Shift ψ for Drift* ($E_0 \neq 0$)

By applying an external electric field we can increase the energy transfer or gain Γ, and the phase shift ψ is increased due to drift. This phase shift is especially large if the transport or Debye length is comparable to or larger than the fringe spacing Λ [11].

The carrier transfer in the initial state of illumination ($t=0$) is described by the diffusion length $L_D=(kT/e\mu\tau)^{1/2}$ and drift length $L_d=\mu\tau E_0$. However, in the stationary state ($t\to\infty$) the carrier transfer is characterized by the Debye length l_D (at $E_0=0$) and by the electric stretch length l_d, respectively [11]. The Debye length calculated for the linear recombination case [11] is given by

$$l_D=\left(\frac{\pi\varepsilon_0\varepsilon_{33}kT}{e^2N_A}\right)^{1/2}=0.5\,\mu m, \tag{9}$$

where $N_A=10^{15}\,cm^{-1}$* is the trap concentration, $\varepsilon_{33}=50$ the dielectric constant [26] and ε_0 the free space permeability. In the similar way [11] we get for the electric stretch length

$$l_d=\frac{\varepsilon_0\varepsilon_{33}}{2eN_A}E_0=1\,\mu m \tag{10}$$

provided $E_0=7\,kV/cm$.

* The value of N_A is determined on the basis of the experimental results of $\eta(\Lambda)$ using the Kukhtarev-Vinetskii theory [11] for the linear recombination case (see below).

The drift length L_d determined by photoelectric measurements is larger than l_d. From the measurements of photocurrent spectra [22] we can obtain an upper bound for the quantum efficiency $\phi \approx 1/3$ (assuming $\phi=1$ for maximal photocurrent at $\lambda=370\,nm$) for $\lambda=488\,nm$ light. Using $\phi=1/3$ and $\phi\mu\tau=1.0\cdot10^{-8}\,cm^2/V$ obtained in our photoconductivity experiments [24] we get for the drift length

$$L_d \geqq \mu\tau E_0=2.1\,\mu m, \quad \text{for} \quad E_0=7\,kV/cm.$$

These considerations confirm the fact that a possible violation of quasi-neutrality must be taken into account.

Since coupling between writing beams occurs, we have to discuss our results with a "dynamic" theory [11, 17–20] which takes into account the possible changes in light intensity distribution during recording. The theory should also be valid for drift and diffusion and for drift or diffusion lengths comparable with the fringe spacing. From the theories mentioned above, only the one from Kukhtarev and Vinetskii [4] applys for long transport lengths. The main results of this theory have been presented in Sect. 1. For the discussion of our results we will make some approximations which are justified by the experimental results for $E_0 \leqq 3\,kV/cm$:

a) small gain $\left(\frac{\Gamma l}{2} \ll 1\right)$

b) small diffraction efficiency $\left(\frac{\pi\cdot\Delta n\cdot l}{\lambda_0\cos\theta_0/2} \ll 1\right)$

c) small diffusion field $(E_T/E_q \ll 1)$.

The steady-state diffraction efficiency (6) then becomes

$$\eta \sim \frac{E_T^2[1+(E_0/E_T)^2]}{1+(E_0/E_q)^2} \tag{11a}$$

and the gain, (3)

$$\Gamma \sim \frac{E_T(1+E_0^2/E_TE_q)}{1+(E_0/E_q)^2}. \tag{11b}$$

From the result presented in Fig. 3 and with (11) we can determine the maximum space-charge field E_q which corresponds to a complete separation of positive and negative charges by one grating period. For large drift length this situation should be nearly fullfilled for small fringe spacing and large electric fields. Therefore we can set $E_0 \approx E_q$ in that domain and we get from (11a) and (5) $\eta \sim E_q^2 \sim \Lambda^2$ which seems to be the case for small fringe spacings and $E_0=7\,kV/cm$ (Fig. 3).

The fitted data for the diffusion field E_T and the maximum space-charge field E_0 are then

$E_q=7\,kV/cm$,

$E_T=1.6\,kV/cm$ for $\Lambda=1\,\mu m$,

and

$E_q = 70\,\mathrm{kV/cm}$,

$E_T = 0.16\,\mathrm{kV/cm}$ for $\Lambda = 10\,\mu\mathrm{m}$.

Thus, the assumption c is well fullfilled, especially for small grating spacings.

With these assumptions and data we have calculated the theoretical dependence $\eta(\Lambda)$, $\Gamma(\Lambda)$, $\eta(E_0)$ and $\Gamma(E_0)$ by means of (3) and (6) (solid lines in Figs 3–6). As is seen in these figures there is a good qualitative agreement between theory and experiment.

The quantitative agreement between experiment and theory is, however, not so good, especially for the diffraction efficiency. The theoretical values of diffraction efficiency are, e.g., by an order of magnitude larger than the experimental ones. The theoretical values for the gain for $\Lambda = 10\,\mu\mathrm{m}$ agree with the experimental ones within experimental errors, but for $\Lambda = 1\,\mu\mathrm{m}$ they are two to four times larger than in the experiment (Fig. 6).

This difference between theoretical and experimental values of η and Γ has two reasons. The first one is that the theory [11] does not take into account any thermal effects in charge transport. E.g., the finite dark conductivity, which can be comparable to photoconductivity, is known [6, 20] to decrease the diffraction efficiency. The second reason might be a possible reduction of the light modulation due to multiple internal reflections at crystal surfaces, causing a decrease of η according to (6). We have noticed that for strong electric fields ($E > 3\,\mathrm{kV/cm}$) the condition $\pi \Delta n l/\lambda_0 \cos\theta_0/2 \ll 1$ is no longer valid, and therefore (6) is, strictly speaking, inapplicable*, since a more general expression (4) applies in this case.

For intermediate electric fields $E_T < E_0 \ll E_q$ which is always the case for large grating spacings (e.g. $\Lambda = 10\,\mu\mathrm{m}$) we get from (11a) and (11b): $\eta \sim E_0^2$ and $\Gamma \sim E_0^2$ (Figs. 5 and 6). In this case the drift length is short compared with the grating spacing and the phase shifted component of the grating does not change. As can be seen from a comparison of Fig. 5 and Fig. 6 the change in gain with E_0^2 is much weaker than the change in diffraction efficiency, since the former is described by the term $2 \cdot \delta \cdot F/E_q$ in (3) and the latter by the term $(\delta F l)^2/2$ in (6). The deviation from $\eta \sim E_0^2$ for $E_0 > 5\,\mathrm{kV/cm}$ for $\Lambda = 10\,\mu\mathrm{m}$ can be explained by a possible trapping center filling.

From (5) we can now calculate the trap concentration N_A for linear recombination

$$N_A = \frac{\varepsilon_{33}\varepsilon_0}{2e}\,\frac{E_q}{\Lambda} \approx 10^{15}\,\mathrm{cm}^{-3}$$

($\varepsilon_{33} = 50$ [26], $\Lambda = 10^{-6}\,\mathrm{m}$, $E_q = 7 \cdot 10^3\,\mathrm{V/cm}$). (12)

* This fact accounts for anomalously large theoretical values of the "diffraction efficiency" ($\eta > 100\,\%$) (Fig. 3).

External electric fields larger than E_q can no longer separate charges, and therefore no increase of the diffraction efficiency and gain is possible.

Therefore both the diffraction efficiency and gain saturate with increasing electric fields E_0 for $\Lambda = 1\,\mu\mathrm{m}$ and $E_0 > 7\,\mathrm{kV/cm}$ (Figs. 5 and 6).

For increased grating spacings the charge separation becomes larger, too, and the diffraction efficiency and gain are increased only if the external field is large enough to complete charge separation ($E_0 \geqq E_q$). Figure 3 shows that for $E_0 = 7\,\mathrm{kV/cm}$ the diffraction efficiency saturates for large grating spacings, since $E_0 \ll E_q \sim \Lambda$ and charge separation is incomplete with this electric field strength.

The gain Γ has been shown to be determined by the phase shift ψ of the holographic grating with respect to the intensity pattern. Therefore $\Gamma(E)$ and $\Gamma(\Lambda)$ are connected with a variation of ψ if the electric field or fringe spacing are changed.

It follows from (4) that for a completely shifted grating (by $\pi/2$) and for $\Gamma l \ll 1$:

$$\eta = \frac{m}{1+m}\left(\frac{\Gamma l}{2}\right)^2 \sim \Gamma^2. \tag{13}$$

Relation (13) is qualitatively well fullfilled for $\eta(\Lambda)$ and $\Gamma(\Lambda)$ at $E_0 = 0$ and $E_0 \approx E_q$ (for $\Lambda < 3\,\mu\mathrm{m}$), (see Figs. 3 and 4). If $E_0 \ll E_q$, which is the case for $\Lambda > 3\,\mu\mathrm{m}$, the expression (11) does not hold any more, because also unshifted components contribute to the diffraction efficiency.

4.3. Light Intensity Dependence of Diffraction Efficiency η and Gain Γ

The intensity ratio dependence of diffraction efficiency $\eta(m)$ shown in Fig. 7 is well described by the first term in (6). As is seen in Fig. 7, the $\eta(m)$ are slightly asymmetric with respect to $m = 1$. This is due to the beam coupling effect which changes light intensity ratio of the two beams asymmetrically. It has been shown that for materials with larger gain Γ (e.g. in $LiNbO_3$ [11]) this asymmetry is much more expressed.

The gain $\Gamma(m)$ shown in Fig. 7b does not agree with the theoretical result presented in (3), since Γ is independent of m in this equation.

The light intensity dependence presented in Fig. 8 is caused by two reasons:

1) The maximum space-charge field E_q, (5), depends on I_0 and

2) the relative contributions of dark- and photoconductivity changes with I_0.

We think that the observed behaviour of $\eta(I_0)$ is explained by the second argument. However, we can use the first argument to show that in $KNbO_3$ the

linear recombination case applies. According to (3) and (6) for the linear recombination case both η and Γ do not change with light intensity. For the quadratic recombination case however $E_q \sim n_0 \sim I_0^{1/2}$, (5), and η becomes independent of I_0 if $E_0 \ll E_q$ and $\eta \sim E_q^2 \sim I_0$ for $E_0 \gg E_q$. The gain Γ then is independent of I_0 for $E_0 \ll E_q$, (3), and $\Gamma \sim I_0^{1/2}$ for $E_0 \gg E_q$. Because both $\eta(I_0)$ and $\Gamma(I_0)$ do not change essentially with E_0 and Λ, we propose, that linear recombination of carrier applies in reduced $KNbO_3$.

4.4. Temperature Dependence of Diffraction Efficiency η and Gain Γ

Thermal transitions have not been reflected in the theory of Kukhtarev and Vinetskii. It has been shown, however [6, 20], that the space-charge field formed by diffusion or drift depends on the ratio n_p/n_d, where n_p and n_d are the carrier concentrations with and without illumination. Therefore we attribute the observed behaviour of $\eta(T)$ due to the changed values of diffusion field E_T and dark- and photoconductivities. Scattering of light has also been observed, especially at higher temperatures which may result in a decrease of fringe pattern contrast. The initial decrease of diffraction efficiency with increasing temperature shown in Fig. 7 could be due to this effect. Scattering of light is much more evident at higher electric fields which explains the larger decrease in $\eta(T)$ for $E_0 = 3\,\mathrm{kV/cm}$. Other reasons for the temperature dependences of η and Γ might be:

1) A possible increase of the parameter δ in (6) since both the electrooptic coefficient r_{33} H31] and $n_3(T)$ [34] are increasing with T.
2) An increase of the diffusion field $E_T \sim T$
3) A decrease of the maximum space-charge field E_q, (5), due to the increase in $\varepsilon_{33}(T)$ [26].

A decrease of n_p/n_d with increasing temperature [24] can both decrease the diffraction efficiency and, for the shift grating, also the gain [6, 20].

Therefore in the temperature range below 120 °C two opposite processes contribute to the diffraction efficiency η and the gain Γ. First a possible *increase* of η and Γ by increased values of δ and E_T and a *decrease* in η and Γ for increased ratios E_T/E_q and decreased ratio n_p/n_d. The result shows that the second process predominates for $E_0 \neq 0$ (Figs. 9 and 10).

In the temperature region above 120 °C the experimantal situation and the understanding of the photorefractive effect is even more complicated. First, the sample can be heated up even if using light pulses ($\tau = 5\,\mathrm{ms}$) and good heat sinks. The temperature within the crystal might be higher than the one at the heat sink which means that the peak in η near 160 °C is effectively near the orthorhombic–tetragonal transition temperature at 215 °C. Pyroelectric effects and also photodomain effects [27] might be possible too; the latter might occur because the coercitive field is also decreased. The elucidation of the behaviour in the phase transition region, however is not clear and requires a further investigation.

Thermal fixing techniques were not successful in stabilizing holograms in these crystals, meaning that either the electronic conductivity is higher than the ionic one, or the fixed holograms are almost completely neutralized during the attempted readout.

Conclusions

The diffraction efficiency and energy transfer have been investigated for reduced $KNbO_3$, a ferroelectric material where the transport length of the charge carriers is comparable to or larger than the grating spacing. The results can be summarized as follows:

1) the stationary energy transfer is changed with the electric field;
2) the direction of energy transfer shows that photogenerated holes have a greater mobility than electrons;
3) the photorefraction and energy transfer are caused by diffusion (at zero applied field) or by drift ($E_0 \neq 0$) of carriers with migration lengths comparable to or larger than the grating spacing;
4) the photovoltaic mechanism gives a negligible contribution to the effects investigated;
5) the experimental diffraction efficiency and gain as a function of grating spacing and electric field are qualitatively described by the theory of Kukhtarev and Vinetskii;
6) the difference between theory and experiment is due to thermal effects which have been neglected in the above theory.

On the basis of the present investigation it is possible to discuss possible improvements of certain properties of $KNbO_3$ for specific applications. The investigated crystal is a typical material for dynamic hologram storage with a much shorter life time than the time constant of intensity transfer between writing beams. Short recording and erasure times are preferred for dynamic holography for the amplification of time varying coherent light beams and images. However, for this application a large gain [14] and a possibility for changing the gain with an electric field are needed. Reduced $KNbO_3$, up to now, is the only material where the stationary energy transfer can be controlled by an external field. From the viewpoint of applications this effect is more beneficial than a transient energy transfer which has recently been discovered in pure and Fe-doped $LiNbO_3$ [14]. However, relative

changes of the gain with respect to changes in the external field are comparatively small in $KNbO_3$. From (3) it follows that the maximum value of gain, obtained by the complete separation of charges ($E_0 \gg E_q$) in an external field is larger than its initial value by the factor $E_q/E_T \sim \Lambda^2$. Therefore the maximal value of gain is determined by the grating spacing. The second possibility of increasing η and Γ is decreasing the dark conductivity. In this case, however, the recording and erasure times become larger, too.

Acknowledgements. The authors gratefully acknowledge the critical reading of the manuscript and valuable remarks made by S.Odulov and N.Kukhtarev.

References

1. J.P.Huignard, F.Micheron, E.Spitz: In *Optical Properties of Solids. New Developments*, ed. by B.O.Seraphin (North-Holland, Amsterdam 1976) pp. 851–992
2. D.L.Staebler: In *Holographic Recording Materials.* Topics in Appl. Phys. **20** (Springer, Berlin, Heidelberg, New York 1977) pp. 101–133
3. R.L.Townsend, J.T.La Macchina: J. Appl. Phys. **41**, 5188–5192 (1970)
4. J.B.Thaxter, M.Kestigian: Appl. Opt. **13**, 913–924 (1974)
5. E.Krätzig, R.Orlowski: Appl. Phys. **15**, 133–139 (1978)
6. P.Günter, F.Micheron: Ferroelectrics **18**, 27–38 (1978)
7. D.von der Linde, A.M.Glass, K.F.Rodgers: Appl. Phys. Lett. **26**, 22–24 (1975)
8. M.Peltier, F.Micheron: J. Appl. Phys. **48**, 4683–3690 (1977) J.P.Huignard, F.Micheron: Appl. Phys. Lett. **29**, 591–593 (1976)
9. K.Megumi, H.Kozuka, M.Kobayashi, Y.Furukata: Appl. Phys. Lett. **30**, 631–633 (1977)
10. D.L.Staebler, J.J.Amodei: J. Appl. Phys. **43**, 1042–1049 (1972)
11. N.Kukhtarev, V.Markov, S.Odulov, M.Soskin, V.Vinetskii: News of Academy of Sciences of USSR, ser. phys. **41**, 811–820 (1977) (In Russian)
12. V.Markov, S.Odulov, M.Soskin: News of Academy of Sciences of USSR ser. phys. **41**, 821–829 (1977) (In Russian)
13. B.Ya.Zeldonitch: Kratkie soobichenija po fizike (Lebedev Physical Institute Letters, Moscow), No. 5, 20–25 (1970) (In Russian)
14. N.Kukhtarev, V.Markov, S.Odulov: Optics Commun. **23**, 338–343 (1977)
15. J.J.Amodei: Appl. Phys. Lett. **18**, 22–24 (1971)
16. L.Young, W.K.Y.Wong, M.L.W.Thewalt, W.D.Cornish: Appl. Phys. Lett. **24**, 264–265 (1974)
17. Y.Ninomiya: J. Opt. Soc. Am. **63**, 1124–1130 (1973)
18. D.W.Vahey: J. Appl. Phys. **46**, 3510–3515 (1975)
19. R.Magnusson, T.K.Gaylord: J. Appl. Phys. **47**, 190–199 (1976)
20. M.G.Moharam, L.Young: J. Appl. Phys. **48**, 3230–3236 (1977)
21. U.Flückiger, H.Arend: J. Cryst. Growth **43**, 406–417 (1978)
22. P.Günter: Ferroelectrics, to be published
23. M.G.Moharam, L.Young: J. Appl. Phys. **47**, 4048–4051 (1976)
24. A.Krumins, P.Günter: Phys. Status Solidi, to be publ.
25. G.A.Alphonse, R.C.Alig, D.L.Staebler, W.Phillips: RCA Rev. **36**, 213–229 (1975)
26. E.Wiesendanger: Ferroelectrics **6**, 263–281 (1974)
27. V.M.Fridkin, A.A.Grekov, P.V.Ionov, A.I.Rodin, E.A.Savchenko, K.A.Mikhailiana: Ferroelectric **8**, 433–435 (1974)
28. N.B.Angert, V.A.Pashkov, N.M.Solovieva: Sov. Phys. JETP **35**, 167–169 (1972)
29. K.Shvarts, P.A.Augustor, A.O.Ozols, A.K.Popelis: Ferroelectrics **22**, 655–658 (1978)
30. A.V.Guinzberg, K.D.Kochev, Yu.S.Kusminov, T.R.Volk: Phys. Status Solidi (a) **29**, 309–314 (1975)
31. P.Günter: Optics Commun. **11**, 285–290 (1974)
32. Y.Ohmori, M.Yamaguchi, K.Yoshino, Y.Inuishi: Japan. J. Appl. Phys. **15**, 2263–2264 (1976)
33. J.Handerek, Z.Wróbel, K.Wójcik, Z.Ujna: Ferroelectrics **18**, 127–129 (1978)
34. E.Wiesendanger: Ferroelectrics **1**, 141–148 (1970)